INTERNATIONAL SOCIETY FOR
SOIL MECHANICS AND
GEOTECHNICAL ENGINEERING

This paper was downloaded from the Online Library of the International Society for Soil Mechanics and Geotechnical Engineering (ISSMGE). The library is available here:

https://www.issmge.org/publications/online-library

This is an open-access database that archives thousands of papers published under the Auspices of the ISSMGE.

The paper was published in the proceedings of the 11th International Conference on Physical Modelling in Geotechnics (ICPMG2026) and was edited by Ioannis Anastasopoulos. The conference was held from June 8th to June 12th 2026 in Zurich, Switzerland.

Proceedings of the 11th ICPMG 2026
11th International Conference on Physical Modelling in Geotechnics
8-12 June 2026, Zurich, Switzerland
© 2026 the Authors

The influence of overconsolidation ratio on cone penetration resistance in sand

Y. Tian
Fugro Marine Geo Consulting, Louvain-la-Neuve, Belgium, Y.tian@fugro.com
Formerly Department of Civil, Environmental and Mining Engineering, University of Western Australia
A. Arafianto, B. M. Lehane
Department of Civil, Environmental and Mining Engineering, University of Western Australia, Perth, Australia
aflizal.arafianto@research.uwa.edu.au, barry.lehane@uwa.edu.au

ABSTRACT: The tip resistance of a penetrometer in overconsolidated (OC) sand has been observed to be greater than that in a normally consolidated (NC) sand at the same density and stress level. While this increase in tip resistance (q_c) is typically attributed to greater in-situ lateral effective stress, relatively few investigations of factors controlling penetrometer resistance in OC sand have been reported. This paper examines the influence of OCR on q_c measurements by conducting CPTs in NC and OC sand samples. Experimental data collected in sands with different OCRs and under various loading conditions are examined. It is shown that, while in-situ lateral stress (σ'_h) is an important determinant for q_c, there is not a unique relationship between q_c, σ'_h and sand relative density (D_r) for all relative densities. This trend was verified in numerical simulations of cone penetration conducted using the Press-Replace Finite Element Method and the hardening soil constitutive model.

1 INTRODUCTION

The Cone penetration test (CPT) is a widely used in-situ testing method that assists site characterization. The relative density (D_r) of coarse-grained soil is typically assessed indirectly from CPT measurements due to difficulties in obtaining undisturbed samples of these materials. The relationship between cone tip resistance (q_c) and D_r is well-known and generally employs the following format:

$$D_r = C_1 ln\,[q_{c1N}/C_2] \tag{1a}$$

$$q_{c1N} = (q_c/p_{atm})/(\sigma'/p_{atm})^n \tag{1b}$$

where C_1 and C_2 are empirical constants, p_{atm}= atmospheric pressure (100kPa), q_{c1N}= stress normalised cone resistance, n= stress level exponent and σ'= effective stress level at the cone tip (which is typically the in-situ vertical effective stress, σ'_v, or the mean effective stress, p').

Best-fit parameters in Equation (1) are usually determined by conducting CPTs in reconstituted sands placed in a calibration chamber or a geotechnical centrifuge. Lunne & Christoffersen (1983) proposed a relationship that uses $\sigma' = \sigma'_v$ and $n = 0.71$ for stress level normalisation with C_1 and C_2 of 0.34 and 16 respectively; while Baldi et al. (1986) adopts the mean effective stress p' as stress at the cone tip, $C_1 = 0.38$, $C_2 = 23$ with $n = 0.55$

Tian & Lehane (2022) proposed the following relationship based on results obtained a calibration chamber in NC silica sand:

$$D_r = 0.36\,ln\,[q_{c1N}/21] \tag{2a}$$

$$q_{c1N} = (q_c/p_{atm})/(\sigma'_v/p_{atm})^{0.7} \tag{2b}$$

Tian & Lehane (2025) subsequently compared Equation (2) with relationships reported in the literature and found good agreement with those developed for application in normally consolidated fine to medium reconstituted silica sand.

The importance of overconsolidation ratio (OCR) was recognized in a range of studies. Kulhawy & Mayne (1990) proposed the following relationship allowing for the effects of OCR and also incorporating corrections for sand age and compressibility:

$$D_r = \{(q_{c1N}/(305C_F))OCR^{-0.18}C_{age}^{0.5}\}^{0.5} \tag{3}$$

where C_F= sand compressibility factor between 0.91&1.09 (higher value for greater compressibility) and C_{age}=1.2+0.05log[t/100], where t is time in years.

Additional studies of cone resistance in overconsolidated sands are presented by Moss et al. (2006) and Roy et al. (2019). These studies highlight the difficulties in establishing simple practical expressions for assessment of D_r from q_c data. Even for typical fine-medium silica sands, there is considerable uncertainty about the relative density dependence of the relationship between cone resistance and stress level.

This paper therefore seeks to extend the database of experimental observations in overconsolidated sands by presenting results from a CPT investigation conducted in reconstituted silica sand, where the OCR was varied between 1 and 10. Numerical simulation of cone penetration conducted using the Press-Replace Finite Element Method and the hardening soil constitutive model is used to assist interpretation.

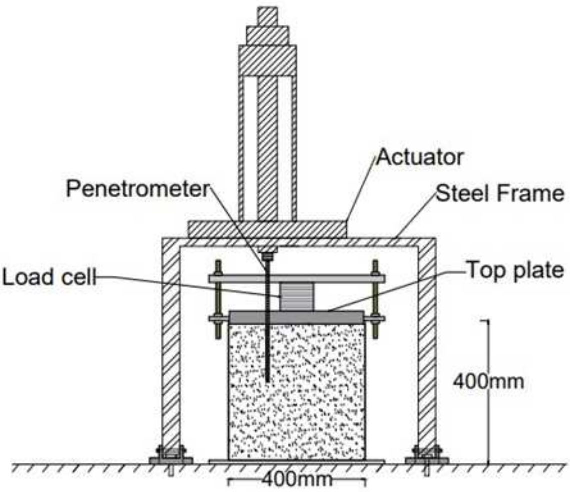

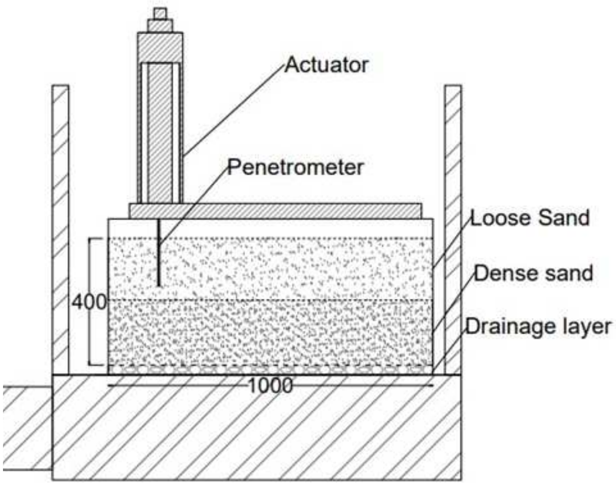

Figure 1. Schematic drawing for (a) calibration chamber tests and (b) centrifuge tests

2 TESTING PROGRAMME

2.1 Soil properties and preparation

The sand employed in the test series is a commercially sourced fine siliceous sand, referred to as UWA sand. The material is of medium angularity with a constant volume friction angle (ϕ'_{cs}) of 31°. It has an average particle size (d_{50}) of 0.18mm and a uniformity coefficient (UC) of 1.4. This sand has been tested extensively at the University of Western Australia (UWA) and its properties are provided in detail in Chow et al. (2019) and Tian & Lehane (2024).

Sand samples were prepared by dry pluviation in calibration chambers or centrifuge strong boxes. To ensure layer uniformity, sand is deposited from a hopper while a constant drop height is maintained. The hopper travels horizontally with a sweeping motion to deposit sand particles evenly inside the chamber. Different relative densities are achieved by varying the horizontal speed, the drop height, and rate of sand flow.

2.2 Overview of experiments performed

CPT were conducted in two different testing environments, namely a calibration chamber and beam geotechnical centrifuge. All CPT conducted were conducted at least 12 cone diameters (12 d_c) away from the sidewall of the chamber/strong box and other testing locations; this distance was previously shown to be sufficient to avoid boundary effects and interference (Tian & Lehane, 2022). The test details are summarised in Table 1 and described below.

Table 1. CPTs presented in this paper

	Chamber Test	
Test Info	**OCR**	**σ'$_v$ [kPa]**
	1	75
d_c=10mm	1.33	75
D_r=0.97	1.5	50
	2	50
	4	25
	Centrifuge Test	
Test Info	**OCR**	**g-level**
d_c=10mm	1	15-50
	Spin up to 100g	
	3	33.3
D_r (loose)=0.3	3.3	30
overlying	5	20
D_r (dense)=0.8	6.7	15
	10	10

2.3 Tests in Calibration Chambers

2.3.1 Test setup

A schematic drawing of the pressure (calibration) chamber setup is shown in Figure 1a. The soil sample awaiting testing sits inside the chamber underneath the actuator. Tests are conducted in NC and OC samples respectively. OC samples were created using pre-consolidation pressure of between 50 and 100kPa followed by unloading to the nominal vertical effective stress (σ'_v). The vertical stress is applied using a horizontal bar with the locking nuts above, and monitored by a loadcell below. An actuator pushes the penetrometer into the sand at a rate of 0.5mm/s.

Centrifuge tests adopt a similar setup except that the specific tests reported here were conducted in two-layer profiles comprising a loose sand layer placed over a dense sand layer.

2.3.2 Test Results

Tip resistance (q_c) measured in uniform NC samples were previously reported by Tian & Lehane (2022), with some typical trends shown in Figure 2a and 2b; these tests clearly show greater q_c values at higher stress levels (σ'_v) and relative density (D_r). Figure 2c shows that use of the normalised cone resistance (q_{c1N}) for the data on Figure 2b leads to a constant q_{c1N} value at all stress levels. These data and other CPTs performed in UWA sand with different D_r and σ'_v values resulted in the best-fit relationship given in Equation (2), which had correlation coefficient r^2 of about 0.95.

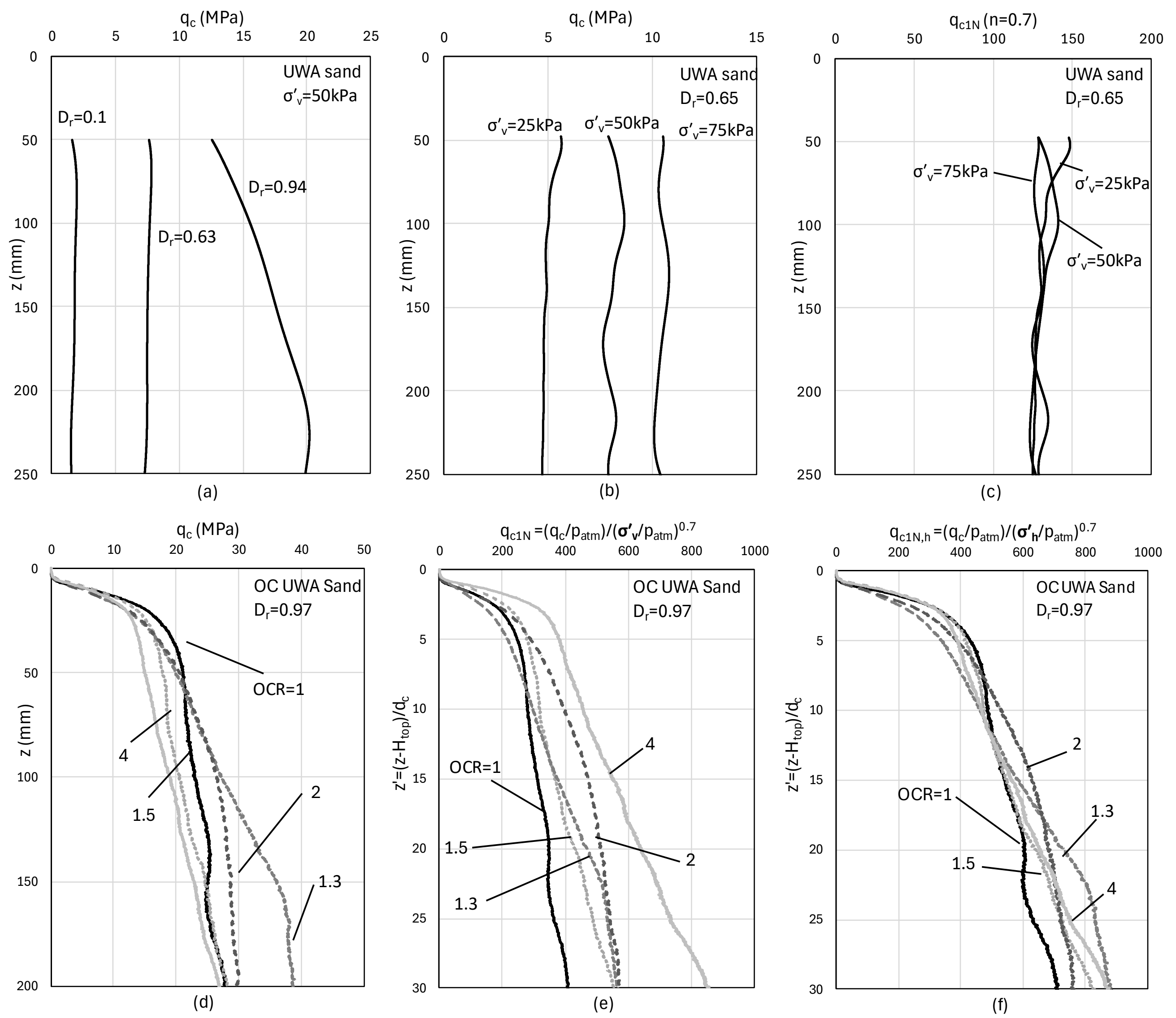

Figure 2. Chamber test results in normally consolidated UWA sand: (a) three D_r tested under σ'_v = 50kPa, (b) D_r = 0.65 tested under different stress level and (c) normalised tip resistance of D_r =0.65. In overconsolidated UWA sand: (d) q_c values and (e) normalised resistance at various OCR, (f) normalised resistance using horizontal stress level (σ'_h)

CPT q_c profiles recorded in very dense UWA sand (D_r=0.97) with OCRs between 1 and 4 are shown in Figure 2d. The normalisation implied by Equation (2) is employed in Figure 2e which plots q_{c1N} profiles for the data plotted on Figure 2d. It is evident that there is a significant spread in the profiles compared with Figure 2c and that use of q_{c1N} to unify tests with the same D_r and σ'_v values is not suitable. This is not unexpected as previous observations have indicated that cone resistance varies more directly with in-situ lateral stress (σ'_h) than vertical stress (Houlsby & Hitchman 1988, Ahmadi & Robertson 2005). The data are therefore re-plotted on Figure 2f using σ'_h for stress normalisation instead of σ'_v where σ'_h is estimated from the expressions of Mayne & Kulhawy (1982), where ϕ'_{cs}=31° for UWA sand:

$$\sigma'_h = (1 - sin\phi'_{cs})/OCR^{sin\phi'_{cs}} \times \sigma'_v \qquad (4)$$

It is seen that the trends at all OCRs are unified, indicating the suitability of employing σ'_h for tip resistance normalisation in OC sands. It is noteworthy, however, that $q_{c1N,h}$ (see definition in Figure 2f) does not stabilise to a steady state value in the very dense sand until the cone reaches a penetration of about 20 to 25d_c. This feature arises because larger development lengths are required in denser sand (e.g. 200mm or 20d_c is required at OCR=1 in Figure 2a). It is also possible that boundary effects due to the high density played a role in the increase in cone resistance at depth in the chamber.

2.4 Tests in the beam centrifuge

While the stress conditions are constant in the calibration chambers, stresses increase with sample depth in centrifuge tests. The rate of increase with depth varies directly with the imposed g-level. Overconsolidation in the centrifuge is induced by spinning the sample at a higher g-level and then reducing the sample at the designated g-level for the CPTs. Close examination does not reveal any differences between stress normalised CPT data recorded in the calilbration chember and centrifuge.

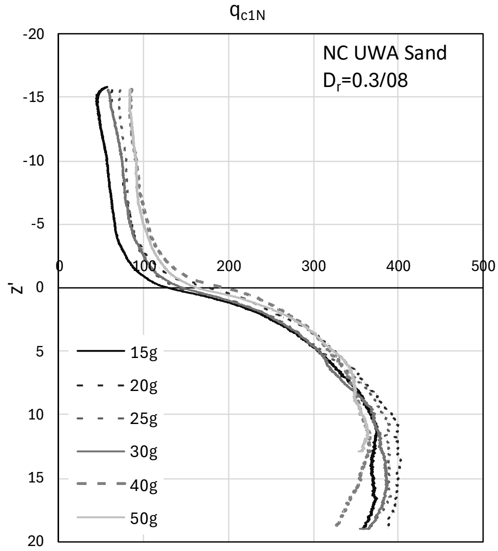

Figure 3. Centrifuge test result in normally consolidated UWA sand under different g-levels

The investigated soil sample comprised a layer of loose sand (D_r = 0.3) overlying a dense sand layer (D_r = 0.8). CPTs were first conducted at OCR=1 at 100g. The g-level was then reduced systematically to induce sample OCRs of between 3 and 10; see Table 1. Samples were allowed to stabilise for 10mins at each g-level before CPTs were performed.

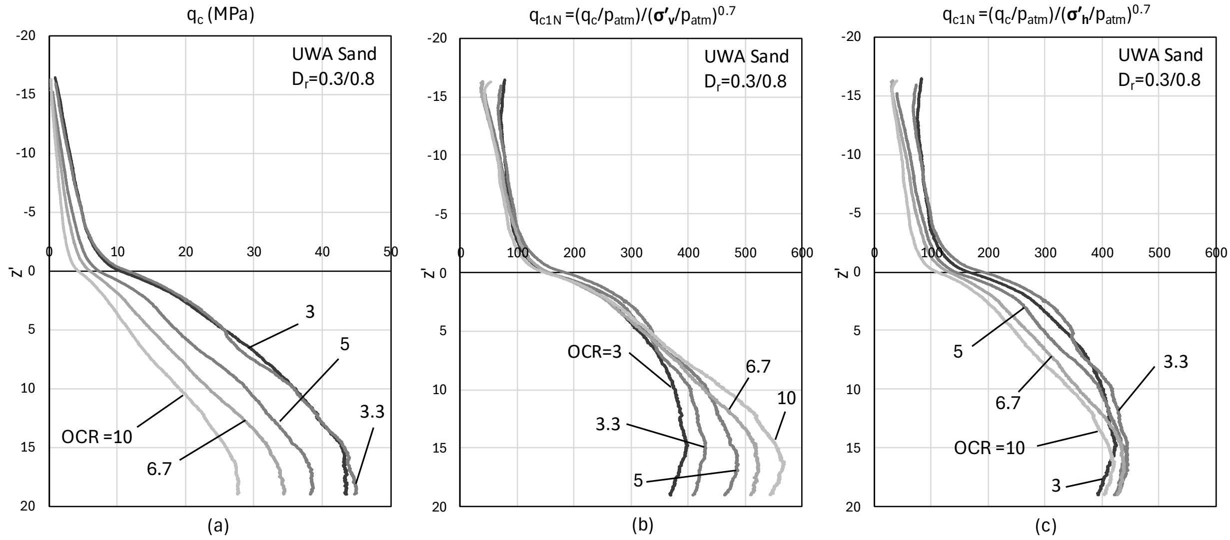

Figure 4. Centrifuge test results in overconsolidated UWA sand (a) obtained q_c measurements (b) normalised tip resistance employing σ'_v and (c) normalised tip resistance employing σ'_h

The CPT data recorded at OCR=1 are plotted in Figure 3 using the normalised cone resistance q_{c1N} (as in Figure 2c and 2e). The transition zone for cone resistance evidently extends from z' =-3 in the loose layer to z' =10 in the dense layer; factors controlling the nature of transition are discussed in Tian & Lehane (2025). Away from the transition zone, it is seen that the normalised cone resistance in the loose sand layer has an approximately constant value of 80 in the loose sand and 350 in the dense sand. These constant values confirm the suitability of the normalised cone resistance term given by Equation 2(b) for a relatively large range in σ'_v values.

Measured resistances for overconsolidated sand samples are shown in Figure 4a and are plotted in normalised from on Figure 4b using q_{c1N} and on Figure 4c using $q_{c1N,h}$. Focusing on data recorded outside the transition zone, it is apparent that use of $q_{c1N,h}$ unifies the cone resistances measured in the dense sand, as seen also for the chamber tests in Figure 2f. However use of q_{c1N} rather than $q_{c1N,h}$ provides a better normalisation in the loose sand. This trend suggests a reduced dependence of q_c on σ'_h in looser sands, which has also been observed by Baldi et al. (1981) and Moss et al. (2006). Further investigations are required to enable a more definitive expression for normalised cone resistance in overconsolidated sands to be deduced. One option would be to allow dependence of the stress level exponent (n) on D_r, as discussed by previous studies (e.g. Salgado & Prezzi 2007, Tian & Lehane 2026). A sensitivity study employing different K_0-OCR relationship is also warrented in future studies to increase the confidence in σ'_h estimations. Insights from numerical investiagtions are presented in the following section.

3 NUMERICAL ANALYSIS

3.1 Modelling approach and analysis overview

To support these experimental observations, CPTs were simulated numerically in finite-element (FE) software using the Press-Replace Method, PRM, (Engin et al. 2015). PRM is a simplified and time-efficient approach for modelling deep penetration problems using small-strain calculations that do not require mesh updates. Penetration is modelled by incrementally pressing the penetrometer into the soil mass and then replacing the displaced soil with the material of the penetrometer. Combined with the appropriate constitutive models and calibrated parameters, this method has been proven to provide reasonable estimates of q_c in different soils (Paniagua et al. 2014, Lim et al. 2018, Arafianto et al. 2021).

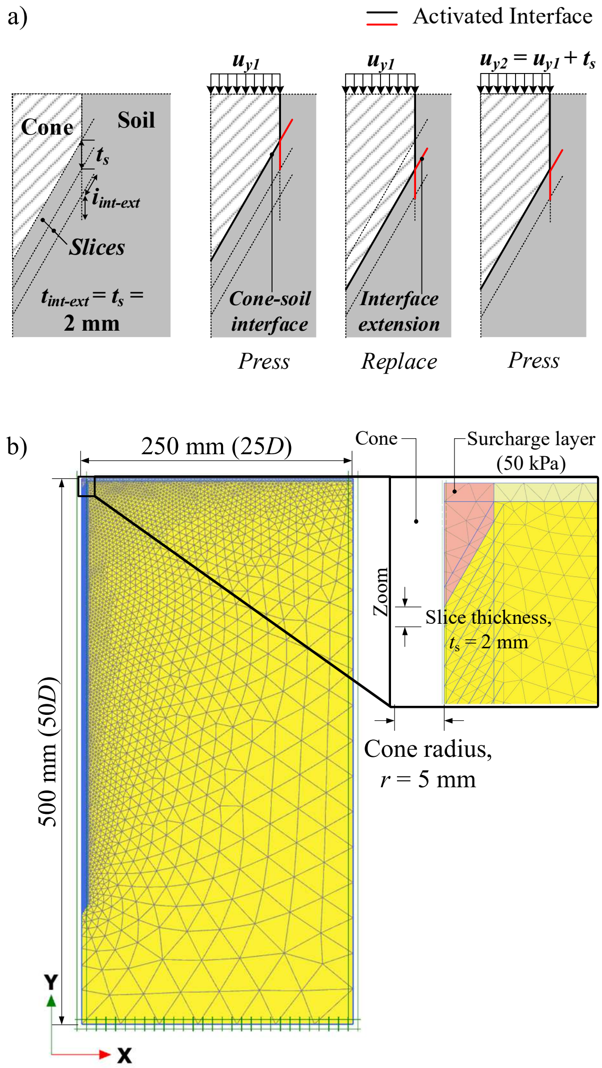

Figure 5. Numerical modelling setup: a) schematic of the Press-Replace Method and b) FE mesh configuration

In this study, the hardening soil (HS) constitutive model (Schanz et al. 1999) was adopted as it enables simulation of CPT responses in sands across a range of relative densities (D_r) and overconsolidation ratios (OCR). Density-dependent behaviour is incorporated through calibrated peak friction (ϕ'_{peak}) and dilatancy angles (ψ), while OCR is defined explicitly as an input parameter. Although the model does not account for fabric evolution, principal stress rotation or strain localisation, it has been demonstrated to provide a satisfactory representation of the macroscopic response governing cone resistance (as described below). The HS model has also been implemented within more advanced numerical frameworks, such as the Material Point Method (MPM) by Martinelli and Galavi (2021), which showed good agreement between predicted and measured CPT end resistances.

To align with observations made from physical modelling, sand of two relative densities is modelled, with $D_r = 0.29$ for loose and $D_r = 0.75$ for dense states.

The HS model was employed with the dilatancy cut-off option enabled. Parameters for the dense sand were derived by Bagbag et al. (2017), and those for loose sand were determined in this study by calibrating against triaxial test data provided in Chow et al. (2019). Table 2 presents the calibrated HS model parameters for both densities.

Table 2. Calibrated HS model parameters for UWA sand

Parameter	Unit	Relative density, D_r (%)	
		29	75
E_{50}^{ref}	kPa	20000	39000
E_{oed}^{ref}	kPa	20000	39000
E_{ur}^{ref}	kPa	60000	117000
ν_{ur}	-	0.2	0.2
m	-	0.65	0.65
p_{ref}	kPa	100	100
c'	kPa	0.1	0.1
ϕ'	°	34	39
ψ	°	2.7	12
$K_{0,NC}$	-	0.5	0.5
R_f	-	0.9	0.9

An illustration of the application of PRM for CPT, along with the overall FE mesh, is shown in Figure 5. An axisymmetric model with a 5 mm cone radius and an apex angle of 60° was implemented. One hundred and fifty cone clusters (*slices*) of 2 mm thickness were preserved, allowing for a maximum of 300 mm penetration. During the penetration phase, a prescribed displacement (u_y) is applied at the top of the cone with cone-soil interfaces and interface extensions at the cone shoulder activated. Next, in the replace phase, the penetrated soil volume is replaced with cone material, and the previous interfaces and their extensions are deactivated (see Figure 5). These press and replace stages are repeated until the desired penetration depth is reached. The cone-soil interfaces were utilised by adopting a strength reduction factor (R_{inter}) of 0.90. To minimise the stress oscillations around the conical tip, interface extensions with very high stiffness and strength were adopted, following the recommendation outlined in Engin (2013).

3.2 Simulation results

CPTs are simulated inside a calibration chamber, where the sample is subjected to a constant vertical stress of 50 kPa. In the FE model, this surcharge was modelled with a 2-mm linear-elastic layer at the top of the mesh. Loose and dense samples with OCR values of 1, 2, and 4 were considered, which correspond to the coefficient of lateral pressure (K_0) of 0.5, 0.7, and 1.0, respectively. For each case, initial stresses were generated with the K_0 procedure, in which the groundwater level was set at the bottom of the model.

The CPT simulations were performed with a pre-embedded cone of 2 mm (see Figure 5) to a total penetration depth of 200 mm. The cone resistances were extracted at 10 mm increments, and best-fit regression lines were generated for each case.

Figure 6 shows the cone resistance profiles predicted for both dense and loose cases. The data points fall around the steady state value as expected. These steady state values are in excellent agreement with measured values, with a difference of only 5% for the dense sand case.

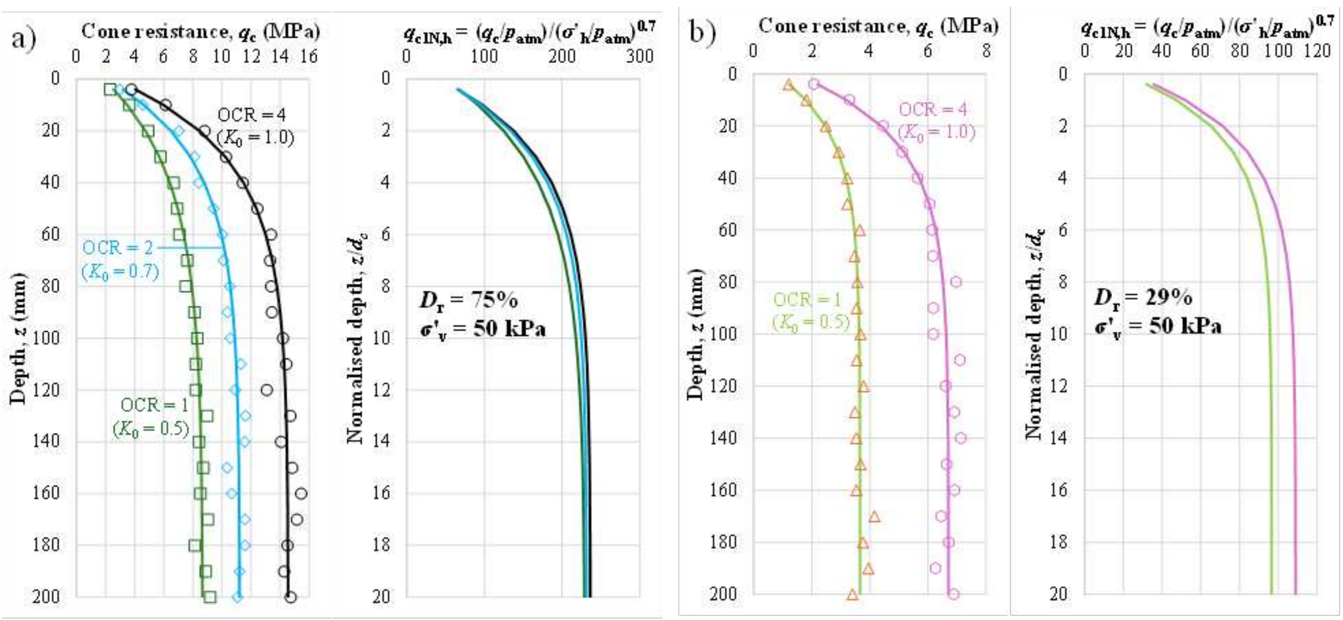

Figure 6. Predicted cone resistance profiles in (a) dense and (b) loose UWA sand

The normalised resistance profiles for the dense sand evidently converge when σ'_h is employed, indicating similar findings to the unique $q_{c1N,h}$ values at a given D_r value seen in the physical tests. For loose sand, however, use of $q_{c1N,h}$ does not lead to exactly the same value at all OCRs, as seen experimentally (Figure 4c). Although different, it is noted that, from a practical point of view, use of $q_{c1N,h}$ can provide an approximate means of unifying cone resistances in sand with different OCRs.

4 CONCLUSIONS

This paper presents data from CPTs conducted in calibration chambers and a geotechnical centrifuge in normally and overconsolidated UWA sand. The test data confirm the strong influence of the in-situ lateral stress (σ'_h) on the cone resistance and support the use of σ'_h rather than σ'_v in empirical expressions relating cone resistance to relative density in overconsolidated sand. Numerical analyses performed using the Press-Replace Finite Element method with the hardening soil model confirm this finding. However, both the experimental and numerical data indicate that the dependence of cone resistance on σ'_h in loose sand is less significant than at higher densities and that additional research is required to optimise empirical formulations. Further investigations into effects of dilatancy, local stress path and critical state soil mechanics through the implementation of other constitutive models could also provide additional insights on the topic.

ACKNOWLEDGEMENTS

The first author acknowledges financial support through the Australian Government Research Training Program (RTP) Scholarship. The second author acknowledges the support from Universitas Katolik Parahyangan, the PhD scholarship from the Ministry of Finance of Indonesia, and the ARC Linkage Project HDR Top-Up Scholarship from the University of Western Australia.

REFERENCES

Ahmadi, M. M., and Robertson, P. K. (2005). Thin-layer effects on the CPT q_c measurement. *Canadian Geotechnical Journal*, 42(5), 1302–1317. https://doi.org/10.1139/t05-036.

Arafianto, A., Rahardjo, P. P., and Lim, A. (2021). Finite-Element Modeling of Cone Penetration in Soft Clay at South Bandung, West Java, Indonesia. *International Journal of Geomechanics*, 21(12), 04021227. https://doi.org/10.1061/(ASCE)GM.1943-5622.0002175.

Baldi, G., Bellotti and R. & Ghionna, V. (1986). Interpretation of CPTs and CPTUs, Part II: Drained Penetration in Sands. In *Proc. Of 4th International Geotechnical Seminar on Field Instrumentation and In Situ Measurements*, Singapore.

Baldi, G., Bellotti, R., Ghionna, V., Jamiolkowski, M. and Pasqualini, E. (1981). Cone resistance in dry NC and OC sands. In *Proc. ASCE Symposium on Cone penetration testing and experience*, St. Louis.

Bagbag, A. A., Lehane, B. M., and Doherty, J. P. (2017). Predictions of footing and pressuremeter response in sand using a hardening soil model. *Proceedings of the Institution of Civil Engineers - Geotechnical Engineering*, 170(6), 479-492.

Chow, S. H., Roy, A., Herduin, M., Heins, E., King, L., Bienen, B., O'Loughlin, C., Gaudin, C., and Cassidy, M. (2019). Characterisation of UWA superfine silica sand. University of Western Australia, Perth.

Engin, H. K. (2013). Modeling Pile Installation Effects: A Numerical Approach. PhD Thesis, TU Delft, Delft.

Engin, H. K., Brinkgreve, R. B. J., and van Tol, A. F. (2015). Simplified numerical modelling of pile penetration – the press-replace technique. *International Journal for Numerical and Analytical Methods in Geomechanics*, 39(15), 1713-1734. https://doi.org/10.1002/nag.2376.

Houlsby, G.T. and Hitchman, R. (1988). Calibration chamber tests of a cone penetrometer in sand. *Geotechnique*, 38(1), pp.39-44.

Kulhawy, F.H. and Mayne, P.W. (1990). Manual on estimating soil properties for foundation design (No. EPRI-EL-6800). Electric Power Research Inst., Palo Alto, CA (USA); Cornell Univ., Ithaca, NY (UWA). Geotechnical Engineering Group.

Lim, Y. X., Tan, S. A., and Phoon, K.-K. (2018). Application of Press-Replace Method to Simulate Undrained Cone Penetration. *International Journal of Geomechanics*, 18(7), 04018066. https://doi.org/10.1061/(ASCE)GM.1943-5622.0001186.

Lunne, T., and H. P. Christoffersen. Interpretation of Cone Penetrometer Data for Offshore Sands. In *Offshore Technology Conference*, pp. OTC-4464. OTC, 1983.

Martinelli, M., and Galavi, V. (2021). Investigation of the Material Point Method in the simulation of Cone Penetration Tests in dry sand. *Computers and Geotechnics*, 130, 103923. https://doi.org/10.1016/j.compgeo.2020.103923.

Mayne, P.W. and Kulhawy, F.H. (1982). K0-OCR relationships in soil. *Journal of the Geotechnical Engineering Division*, 108(6), pp.851-872.

Moss, R. E. S., Seed, R. B., and Olsen, R. S. (2006). Normalizing the CPT for Overburden Stress. *Journal of Geotechnical and Geoenvironmental Engineering*, 132(3), 378–387. https://doi.org/10.1061/(ASCE)1090-0241(2006)132:3(378).

Paniagua, P., Nordal, S., and Engin, H. K. (2014). Back calculation of CPT tests in silt by the Press-Replace technique. *8th European Conference on Numerical*

Methods in Geotechnical Engineering (NUMGE 2014), M. A. Hicks, R. B. J. Brinkgreve, and A. Rohe, eds. Delft, The Netherlands, 391-396.

Roy, A., Chow, S., O'Loughlin, C., and Randolph, M. (2019). Effect of Stress History and Shallow Embedment on Centrifuge Cone Penetration Tests in Sand. *Proceedings of the ASME 38th International Conference on Ocean, Offshore and Arctic Engineering (OMAE2019)*, Paper No. OMAE2019-95393, V001T10A020. ASME. https://doi.org/10.1115/OMAE2019-95393.

Schanz, T., Vermeer, P. A., and Bonnier, P. G. (1999). The hardening soil model: Formulation and verification. *Beyond 2000 in Computational Geotechnics*, Routledge.

Salgado, R. and Prezzi, M. (2007). Computation of cavity expansion pressure and penetration resistance in sands. *International Journal of Geomechanics*, 7(4), 251-265. https://doi.org/10.1061/(ASCE)1532-3641(2007)7:4(251).

Tian, Y., and Lehane, B.M. (2022). Parameters Affecting the CPT Resistance of Reconstituted Sands. In *Cone Penetration Testing 2022*, 734–40. CRC Press. https://doi.org/10.1201/9781003308829-108.

Tian, Y., and Lehane, B.M. (2024). Investigation of the relationship between CPT cone resistance and friction angle for a range of granular soils. In *Proceedings of the 7th International Conference on Geotechnical and Geophysical Site Characterization*.

Tian, Y. and Lehane, B.M. (2025). The influence of soil layering and penetrometer diameter on penetration resistance. *Canadian Geotechnical Journal*. https://doi.org/10.1139/cgj-2024-0491.

Tian, Y. and Lehane, B.M. (2026). An experimental investigation of factors affecting drained CPT resistance in normally consolidated granular materials. *Canadian Geotechnical Journal.* https://doi.org/10.1139/cgj-2025-0697.